Direct Determination of Dynamic Properties of Coulomb and Yukawa Classical One-Component Plasmas

Yu. V. Arkhipov, A. Askaruly, A. E. Davletov, and D. Yu. Dubovtsev
Al-Farabi Kazakh National University, IETP, Faculty of Physics and Technology, al-Farabi 71, 050040 Almaty, Kazakhstan

Z. Donkó, P. Hartmann, and I. Korolov
Institute of Solid State Physics and Optics, Wigner Research Centre for Physics, Hungarian Academy of Sciences, P.O. Box 49, 1525 Budapest, Hungary

L. Conde
Departamento de Física Aplicada a la Ingeniería Aeronáutica, ETSIA, Universidad Politécnica de Madrid, Pl. Cardenal Cisneros 3, 28040 Madrid, Spain

I. M. Tkachenko*
Departamento de Matemática Aplicada, Universidad Politécnica de Valencia, Camino de Vera s/n, 46022 Valencia, Spain
(Received 8 September 2016; published 27 July 2017)

Dynamic characteristics of strongly coupled classical one-component Coulomb and Yukawa plasmas are obtained within the nonperturbative model-free moment approach without any data input from simulations so that the dynamic structure factor (DSF) satisfies the first three nonvanishing sum rules automatically. The DSF, dispersion, decay, sound speed, and other characteristics of the collective modes are determined using exclusively the static structure factor calculated from various theoretical approaches including the hypernetted chain approximation. A good quantitative agreement with molecular dynamics simulation data is achieved.

DOI: 10.1103/PhysRevLett.119.045001

Strongly coupled plasmas (SCPs) appear in various settings in nature (e.g., in dense astrophysical matter in white dwarfs and neutron stars [1]), as well in the laboratory (in ultracold plasmas [2], electrolytes and charged stabilized colloids [3], laser-cooled ions in cryogenic traps [4], and dusty plasmas [5]). SCPs and warm dense matter are highly relevant model systems for inertial fusion devices [6]. The common property of SCPs is that the interparticle potential energy dominates over the thermal energy. Many of the above-mentioned systems have been analyzed and their characteristic effects became understood within the framework of a seminal model system, the one-component plasma (OCP) model that considers explicitly only one type of charged species, while the presence and the effects of other charged species are expressed by the interaction potential $\varphi(r)$.

SCPs, as many-body dynamical systems, exhibit various collective excitations, of which the properties have been investigated both via theoretical approaches and numerical simulations. Numerical approaches provide direct access to the central quantity of collective effects, the dynamic structure factor (DSF). The most successful theoretical approach capable of describing strongly coupled plasmas, the quasilocalized charge approximation [7], is able to predict [from the static pair distribution function (PDF)] the dispersion relations of the collective modes; however, it cannot predict the lifetime (decay) of the modes and the form of the DSF itself. Here we demonstrate that the method of moments theoretical approach [8] is able to predict the form and structure of the DSF of the OCP, based on static data only, i.e., the PDF or the static structure factor (SSF). As both the PDF and the SSF can be obtained theoretically as well [e.g., within the hypernetted chain (HNC) approximation and its modifications including the bridge function] the present approach provides a purely theoretical access to the full DSF and a full quantitative description of the collective modes, including their decay and other characteristics, without the necessity to use simulation data as input, as it was done in [9,10].

The moment approach is nonperturbative, nonparametric, and model free. Thus it is perfectly applicable to a broad class of fluids characterized by response functions like semidegenerate multicomponent Coulomb systems or even simple liquids. Because of the rigorous mathematical background, the method is based on automatic satisfaction of sum rules and other exact relations. An empirical guidance is plugged directly into the intermediate step of theoretical computations, thus closing the approach and permitting us, in addition, to determine the dynamic characteristics in terms of the static ones. OCPs are chosen in this Letter for the demonstration of the numerical validity of the approach. Results for other types of fluids are to be presented elsewhere.

Two main types of potentials are of interest in OCPs. The Coulomb potential describes systems where the background

of the oppositely charged species is not polarizable (e.g., a degenerate electron liquid embedding positive ions)—systems with this property are further referred to as Coulomb OCPs (COCPs), while the Yukawa OCPs (YOCPs) are characterized by a screened-Coulomb (Debye-Hückel, or Yukawa) potential between the "primary" species, where the screening is established by "secondary" species.

From the point of view of statistics, the OCPs we consider here are classical systems; no quantum effects are taken into account. Hence, all properties of COCPs characterized by $\varphi_C(r) = (Ze)^2/r$ depend on a unique dimensionless coupling parameter $\Gamma = \beta(Ze)^2/a$. Here β^{-1} stands for the temperature in energy units, Ze denotes the particle charge, and $a = (3/4\pi n)^{1/3}$ is the Wigner-Seitz radius, n being the number density of the particles. The strongly coupled (liquid) domain is characterized by $\Gamma > 1$. The upper limit of the coupling parameter for the liquid phase is determined by the Wigner crystallization into Coulomb crystals [11].

In YOCPs, in addition to the coupling parameter Γ, the screening is expressed by the parameter κ that "tunes" the range of the interaction potential, $\varphi_Y(r) = ((Ze)^2/r)\exp(-\kappa r/a)$.

For convenience, we introduce here the dimensionless wave number $q = ka$ and write the Fourier transforms of both potentials in terms of the form factor: $\varphi_\alpha(q) = 4\pi(Zea/q)^2\zeta_\alpha(q;\kappa)$, $\alpha = C, Y$. In YOCPs, $\zeta_Y(q,\kappa) = q^2/(q^2+\kappa^2)$, while in Coulomb OCPs $\zeta_C(q;\kappa=0) = 1$. The crystallization condition of the YOCPs depends on both parameters [12]. The chief dynamic characteristic of the systems we consider here is the DSF, $S(q,\omega;\kappa)$, which is a positive even function of frequency. The dimensionless even-order power frequency moments of the DSF,

$$S_\nu(q;\kappa) = \frac{1}{n}\int_{-\infty}^{\infty}\omega^\nu S(q,\omega;\kappa)d\omega, \quad \nu = 0,2,4,$$

are the known sum rules (see [13,14], and references therein),

$$\begin{aligned}
&S_0(q;\kappa) = S(q;\kappa), \qquad S_2(q) = \frac{\omega_p^2 q^2}{3\Gamma},\\
&S_4(q;\kappa) = \omega_p^2 S_2(q)[\zeta_\alpha(q;\kappa) + q^2/\Gamma + U(q;\kappa)],\\
&U(q;\kappa) = \frac{1}{12\pi}\int_0^\infty [S(p;\kappa)-1]f(p,q;\kappa)p^2dp,\\
&f(p,q;\kappa) = \frac{2(3q^2-\kappa^2-p^2)}{q^2} + \frac{(q^2-\kappa^2-p^2)^2}{2q^3p}\\
&\qquad\times\ln\left(\frac{\kappa^2+(q+p)^2}{\kappa^2+(q-p)^2}\right) - \frac{8p^2}{3(\kappa^2+p^2)}.
\end{aligned} \tag{1}$$

The odd-order moments vanish due to the symmetry of the DSF. Contrary to the multicomponent plasma situation [15], higher-order OCP sum rules converge but they are related to scarcely studied nonpairwise correlations that we neglect here; see nevertheless [16]. Notice that

$$\begin{aligned}
U(q\to 0;\kappa) &\simeq \frac{4q^2}{45\pi}\int_0^\infty \frac{(1+\frac{5\kappa^2}{2p^2}+\frac{15\kappa^4}{2p^4})}{(1+\frac{\kappa^2}{p^2})^3}[S(p;\kappa)-1]dp\\
&= \frac{4q^2}{45\Gamma}u(\Gamma,\kappa) + O(q^4),
\end{aligned} \tag{2}$$

where $u(\Gamma,\kappa)$ is the correlation energy per particle normalized to the temperature [17]; $\omega_p^2 = 3e^2/ma^3$ is the plasma frequency and $S(q;\kappa)$ is the static structure factor.

The Nevanlinna formula of the classical theory of moments [8] establishes a unilateral correspondence between the DSF (as a noncanonical solution of the moment problem) and the nonphenomenological Nevanlinna parameter function (NPF) $Q(q,\omega = \mathrm{Re}z + i0^+;\kappa)$ which additionally satisfies the following limiting condition [8]: $\lim_{z\to\infty}[Q(q,z;\kappa)/z] = 0$, $\mathrm{Im}z > 0$,

$$\frac{\pi S(q,\omega;\kappa)}{nS(q;\kappa)} = \frac{\omega_1^2(\omega_2^2-\omega_1^2)\mathrm{Im}Q}{|\omega(\omega^2-\omega_2^2)+Q(\omega^2-\omega_1^2)|^2}, \tag{3}$$

where the characteristic frequencies are defined by the ratios of the moments: $\omega_1^2(q;\kappa) = S_2(q)/S(q;\kappa)$, $\omega_2^2(q;\kappa) = S_4(q;\kappa)/S_2(q)$.

Consider a canonical solution of the moment problem [18] corresponding to the set $\{S_0(q;\kappa),0,S_2(q),0,S_4(q;\kappa)\}$,

$$\frac{S(q,\omega;\kappa)}{nS(q;\kappa)} = \left(1-\frac{\omega_1^2}{\omega_2^2}\right)\delta(\omega) + \frac{\omega_1^2}{2\omega_2^2}[\delta(\omega-\omega_2)+\delta(\omega+\omega_2)]. \tag{4}$$

Notice that due to the Cauchy-Schwarz inequality [14,19], $\omega_1^2(q;\kappa) < \omega_2^2(q;\kappa)$. The Feynman-like [20] solution (4) describes nondecaying collective modes in the system: a diffusive one at $\omega = 0$, as well as an optical (plasma or Langmuir-Bohm-Gross) mode at $\omega_L = \omega_2(q;\kappa=0)$ in the COCPs and a quasiacoustic mode in the YOCPs with the sound velocity

$$c_s(\kappa) = \omega_p\sqrt{\frac{1}{\kappa^2} + \frac{4u(\Gamma,\kappa)+45}{45\Gamma}}. \tag{5}$$

This mode exhibits a roton minimum at higher q values, attributable to the quasilocalization of particles in a strongly correlated liquid [21]. Because of the compressibility sum rule and Parseval's identity, the correlation energy $u(\Gamma,\kappa)$ is directly related to the system compressibility.

In the present work, we do not reconstruct the NPF from the very data we wish to describe like it was done in [22], but model it by its static value [9,10]: $Q(q,\omega;\kappa) = Q(q,0;\kappa) = ih(q;\kappa)$, $h(q;\kappa) > 0$. The latter positive parameter function was related in [10] to the static value of the DSF directly via (3). Here we suggest determining it independently on the basis of the empirical observation that the DSFs exhibit extrema at $\omega = 0$. Because of its symmetry, the DSF

$$\left.\frac{\pi S(q,\omega;\kappa)}{nS(q;\kappa)}\right|_{Q=ih} = \frac{\omega_1^2(\omega_2^2-\omega_1^2)h}{\omega^2(\omega^2-\omega_2^2)^2+h^2(\omega^2-\omega_1^2)^2} \quad (6)$$

depends only on the square of frequency. The rhs of (6) as a function of a new variable $x=\omega^2$ is proportional to

$$F(x;h) = (x(x-\omega_2^2)^2 + h^2(x-\omega_1^2)^2)^{-1},$$

which exhibits extrema at $x=0$ if $F'(0;h) = (2h^2\omega_1^2-\omega_2^4)/h^4\omega_1^8 = 0$, i.e., if

$$h(q;\kappa) = h_0(q;\kappa) = \frac{\omega_2^2(q;\kappa)}{\sqrt{2}\omega_1(q;\kappa)}, \quad (7)$$

while the sign of the second derivative at $x=0$ for $h=h_0$, $F''(0;h_0) = 4(4\omega_1^2-\omega_2^2)/(\omega_1\omega_2)^6$, i.e., the sign of the parameter $\theta = (2\omega_1-\omega_2)/\omega_p \in (-\omega_2/\omega_p, \omega_2/\omega_p)$ determines the nature of the extremum at $\omega=0$. A positive $\theta(q;\kappa)$ corresponds to a minimum, and vice versa. Notice that the DSF value at $\omega=0$,

$$\left.\frac{\pi S(q,0;\kappa)}{nS(q;\kappa)}\right|_{Q=ih} = \frac{\omega_2^2(q;\kappa)-\omega_1^2(q;\kappa)}{h(q;\kappa)\omega_1^2(q;\kappa)},$$

is positive and observe that $S(q,0;\kappa)$ for $h=h_0$ is a decreasing function of the parameter $\theta(q;\kappa)$. It is important that here we do not rely on adjustable parameters like $S(q,0;\kappa)$, and that the resulting expression,

$$\frac{\pi S(q,\omega;\kappa)}{nS(q;\kappa)} = \frac{\omega_1^2(\omega_2^2-\omega_1^2)h_0}{\omega^2(\omega^2-\omega_2^2)^2+h_0^2(\omega^2-\omega_1^2)^2}, \quad (8)$$

contains no static parameters, which we could not calculate theoretically or numerically. In other words, given the thermodynamic parameters of the system or the values of the coupling and screening parameters Γ and κ, we are able to predict the form of the DSF by calculating only the static characteristics of the system. Besides, the position of the shifted maximum in the spectrum, which is the COCP Langmuir-Bohm-Gross mode frequency or the YOCP acoustic-roton mode frequency, can be calculated directly as an exact solution of the dispersion equation

$$z[z^2-\omega_2^2(q;\kappa)] + ih_0(q;\kappa)[z^2-\omega_1^2(q;\kappa)] = 0. \quad (9)$$

To this end the solutions of this equation found in [10] can be employed, particularly the one corresponding to the "shifted" mode: $\omega_{\rm sh}(q,\kappa) = \omega(q,\kappa) - i\delta(q,\kappa) = -wX - w^2Y - ih_0/3$, where $w = \exp(2\pi i/3)$,

$$X = \sqrt[3]{h_0W/2i + Z^3}, \qquad Y = \sqrt[3]{h_0W/2i - Z^3},$$
$$Z^3 = \sqrt{-(\omega_2^2/3 - h_0^2/9)^3 - (h_0W/2)^2},$$
$$W = -\omega_2^2/3 + \omega_1^2 + 2h_0^2/27. \quad (10)$$

In the following we present the results obtained via the theoretical approach described above and compare these with the results of numerical simulations.

Our molecular dynamics (MD) code simulates the motion of $N = 10\,000$ pointlike particles within a cubic cell. For the COCP case we use the particle-particle particle-mesh method to account for the long range of the Coulomb potential [23], while for the YOCP the fast decay of the interaction forces makes it possible to introduce a cutoff distance, beyond which the interaction of particle pairs can be neglected. The integration of the equations of motion is performed with the velocity-Verlet scheme. At the initialization of the simulations the positions of the particles are set randomly, while their initial velocity vectors are sampled from a Maxwellian distribution corresponding to a specified system temperature. During the first phase of the simulations the particle velocities are rescaled in each time step, in order to reach the desired temperature. This procedure is stopped before the second, measurement phase of the simulation, when data are collected for the spatial Fourier components of the microscopic density, and an additional Fourier transform in the time domain yields the DSF.

In Figs. 1 and 2 we display results for the DSFs of the COCP and YOCP, respectively, compared to the simulation data. These and other results displayed here were obtained using the SSF calculated within the HNC approximation. We have studied the dependence of the quality of our dynamic results on the method of precalculation of the SSF. Up to seven different static approaches were analyzed; certain minor improvements (up to 5%) were observed with respect to the HNC; see details in Supplemental Material [24].

A fairly good agreement is observed not only in the above figures, but in all cases we have considered; see Supplemental Material [24]. We believe that the present approach can be extended to the whole OCP liquid plane. A similar level of overall agreement with the MD data has

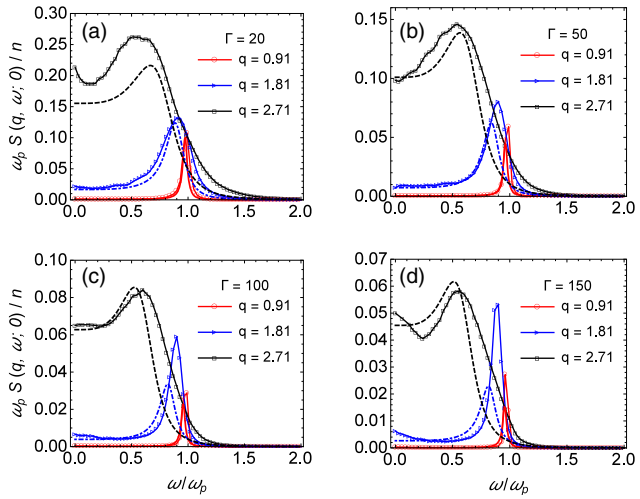

FIG. 1. The COCP DSF calculated from (8) (lines) and obtained from MD simulations (symbols).

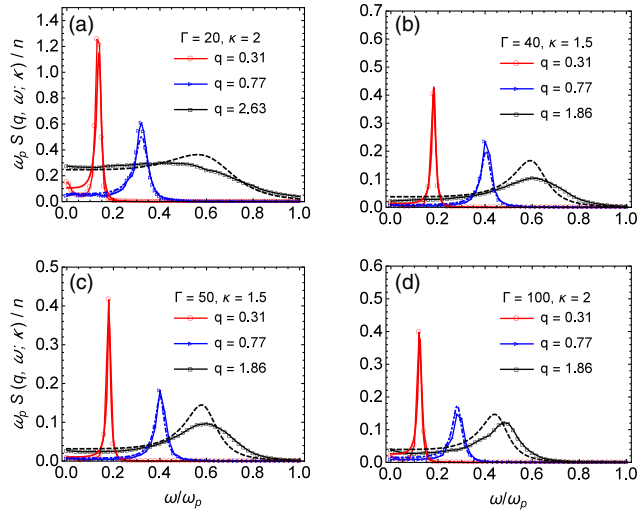

FIG. 2. The YOCP DSF calculated from (8) (lines) and obtained from MD simulations (symbols).

been achieved only by direct adjustment [33]. The parameter $\theta(q;\kappa)$ conveys important information about the decay of the collective mode: positive values indicate propagating (weakly decaying) modes, while at negative values energy dissipation processes prevail; see, e.g., Fig. 3.

When the collective mode is weakly decaying, we can predict the characteristics of the mode: the dispersion of the Langmuir-Bohm-Gross mode in COCPs and of the quasiacoustic mode in YOCPs; we can also calculate the sound speed in the latter with fairly high precision; see Figs. 4 and 5.

The roton parabolic minima become well pronounced in the YOCP collective mode dispersion curves at higher values of the wave number and the coupling parameter Γ,

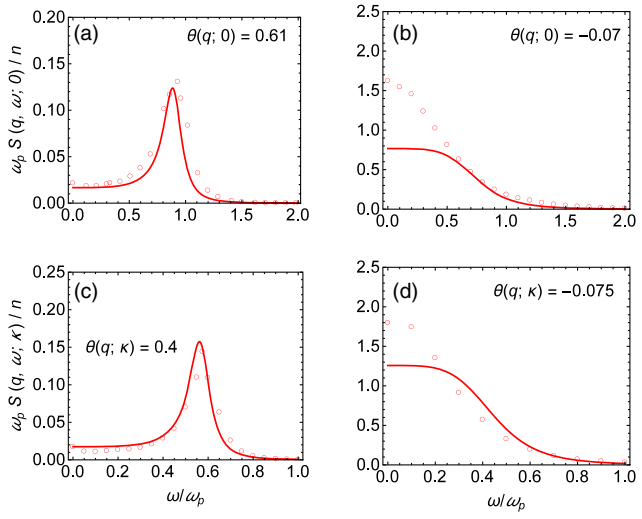

FIG. 3. The COCP DSF at $\Gamma = 20$ [(a) and (b)] and YOCP DSF at $\Gamma = 40$, $\kappa = 1.5$ [(c) and (d)] calculated from (8) (lines) and obtained from MD simulations (circles); (a) $q = 1.8$, (b) $q = 4.7$, (c) $q = 1.39$, and (d) $q = 4.02$.

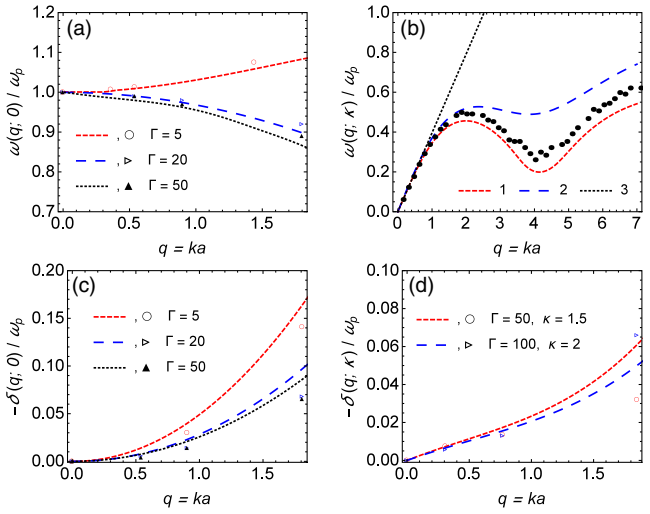

FIG. 4. (a) Dispersion relation for the COCP plasma modes, compared to MD data. Lines correspond to the exact solution of (9). (b) Dispersion relation for the YOCP quasiacoustic mode at $\Gamma = 100$ and $\kappa = 2$, compared to MD data. 1 stands for the exact solution of (9), 2 represents $\omega_2(q;\kappa)$, and 3 is the acoustic part of the mode, $\omega = c_s q$. (c) Decrement of the COCP plasma modes. (d) Decrement of the YOCP acoustic modes. Lines stand for the exact solutions with HNC SSFs; dots were derived as the full width at half maximum of the MD DSF.

and as the screening parameter a/κ approaches the Wigner-Seitz radius a or $\kappa \to 1$ [21]. The negative dispersion is, certainly, observed for the COCP optical mode for $\Gamma \gtrsim 9$ when the negative correlation contribution to the fourth sum rule (1), $U(q;0)$, compensates the kinetic one. In COCPs we also observe a significantly decaying plasmon-roton mode.

Notice that when $\theta(q;\kappa)$ is positive we can even predict the decrement of the propagating mode with an acceptable precision. When $\theta(q;\kappa) < 0$ the "shifted" mode merges with the "unshifted" diffusive mode and we can no longer assign the imaginary parts of the solutions of Eq. (18) to different modes.

In conclusion, a theoretically rigorous and computationally efficient nonphenomenological algorithm with no perturbative or adjustment parameters is proposed for the straightforward calculation of various dynamic

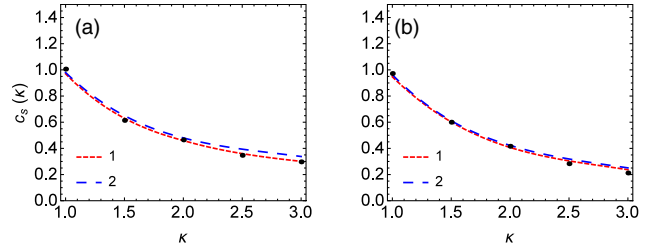

FIG. 5. Sound speed in YOCPs for (a) $\Gamma = 20$ and (b) $\Gamma = 100$, compared to the MD results (dots). 1 was calculated using HNC or any other SSF, and 2 corresponds to (5).

characteristics of classical strongly coupled Coulomb and Yukawa fluid OCPs in terms of the static structure factors of these systems only. The latter were calculated using the HNC. A parameter allowing for a discrimination between propagating and strongly decaying collective modes was introduced. Thus, we are able to predict the form and provide a reliable numerical outcome for the DSFs with no adjustment to the dynamical data. A good agreement is obtained with available numerical data on other dynamic characteristics like the collective mode dispersion in COCPs, the acoustic-roton mode, and the sound speed in YOCPs. Additional graphical material, in particular, obtained with the MD and alternative static schemes, and other details are provided in Supplemental Material [24].

In the context of the inverse dielectric function, the present method can also be employed for the solution of other dynamic problems, like the reflectivity or the stopping power and straggling in more complex systems, which is a work in progress. In general, the suggested mathematical approach is perfectly applicable in any physical system described by a response function like the inverse dielectric function or the DSF, as it was intended in [34–36] but still with the involvement of the simulation data.

This research work was supported by Grants No. 0263/PTsF, No. 3119/GF4, No. 3120/GF4, and No. 3831/GF4 (Ministry of Education and Science, Kazakhstan), No. NKFIH 119357 and No. 115805 (National Research, Development and Innovation Fund, Hungary), the János Bolyai Research Scholarship of the Hungarian Academy of Sciences (P. H.), Hungary, and Grant No. ESP2013-41078R (Ministerio de Economía y Competitividad, Spain). A. A. expresses gratitude for the financial support provided by the grant "The best lecturer of the Republic of Kazakhstan," and I. M. T. acknowledges the hospitality of the al-Farabi Kazakh National University and valuable discussions with M. Bonitz, I. L. Iosilevskiy, and Yu. A. Serebrennikov. Special thanks are due to Kh. Santybayev, who has helped us with the analysis of alternative approaches to the calculation of the SSF.

*imtk@mat.upv.es

[1] S. Ichimaru, Rev. Mod. Phys. **65**, 255 (1993); *The Equation of State in Astrophysics*, edited by G. Chabrier and E. Schatzman (Cambridge University Press, Cambridge, 1994).

[2] T. C. Killian, T. Pattard, T. Pohl, and J. M. Rost, Phys. Rep. **449**, 77 (2007); M. Yan, B. J. DeSalvo, Y. Huang, P. Naidon, and T. C. Killian, Phys. Rev. Lett. **111**, 150402 (2013).

[3] S. Alexander, P. M. Chaikin, P. Grant, G. J. Morales, P. Pincus, and D. Hone, J. Chem. Phys. **80**, 5776 (1984); K. Kremer, M. O. Robbins, and G. S. Grest, Phys. Rev. Lett. **57**, 2694 (1986).

[4] S. L. Gilbert, J. J. Bollinger, and D. J. Wineland, Phys. Rev. Lett. **60**, 2022 (1988); M. G. Raizen, J. M. Gilligan, J. C. Bergquist, W. M. Itano, and D. J. Wineland, Phys. Rev. A **45**, 6493 (1992); D. H. E. Dubin and T. M. O'Neill, Rev. Mod. Phys. **71**, 87 (1999).

[5] H. Ohta and S. Hamaguchi, Phys. Rev. Lett. **84**, 6026 (2000); G. Kalman, M. Rosenberg, and H. E. DeWitt, Phys. Rev. Lett. **84**, 6030 (2000); P. K. Kaw and A. Sen, Phys. Plasmas **5**, 3552 (1998); M. S. Murillo, Phys. Rev. Lett. **85**, 2514 (2000).

[6] M. S. Murillo, Phys. Plasmas **11**, 2964 (2004); V. Fortov, I. Iakubov, and A. Khrapak, *Physics of Strongly Coupled Plasma* (Oxford, Clarendon Press, 2006); F. Graziani, M. P. Desjarlais, R. Redmer, and S. D. B. Trickey, *Frontiers and Challenges in Warm Dense Matter* (Springer, Berlin, 2014).

[7] K. I. Golden and G. J. Kalman, Phys. Plasmas **7**, 14 (2000); **8**, 5064 (2001).

[8] M. G. Krein and A. A. Nudel'man, *The Markov Moment Problem and Extremal Problems*, Translations of Mathematical Monographs (American Mathematical Society, Providence, 1977), Vol. 50; V. M. Adamyan, T. Mayer, and I. M. Tkachenko, Fiz. Plazmy **11**, 826 (1985) Sov. J. Plasma Phys. **11**, 481 (1985)]; I. M. Tkachenko, Yu. V. Arkhipov, and A. Askaruly, *The Method of Moments and its Applications in Plasma Physics* (LAP Lambert Academic Publishing, Saarbrücken, 2012) and references therein.

[9] S. V. Adamyan, T. Meyer, and I. M. Tkachenko, Contrib. Plasma Phys. **29**, 373 (1989).

[10] Yu. V. Arkhipov, A. Askaruly, D. Ballester, A. E. Davletov, I. M. Tkachenko, and G. Zwicknagel, Phys. Rev. E **81**, 026402 (2010).

[11] H. M. Van Horn, Phys. Lett. A **28**, 706 (1969); J. P Hansen, Phys. Lett. A **41**, 213 (1972); H. Ikezi, Phys. Fluids **29**, 1764 (1986); H. Thomas, G. E. Morfill, V. Demmel, J. Goree, B. Feuerbacher, and D. Möhlmann,, Phys. Rev. Lett. **73**, 652 (1994).

[12] G. Faussurier, Phys. Rev. E **69**, 066402 (2004).

[13] A. A. Kugler, J. Stat. Phys. **8**, 107 (1973); K. N. Pathak and P. Vashishta, Phys. Rev. B **7**, 3649 (1973).

[14] Yu. V. Arkhipov, A. B. Ashikbayeva, A. Askaruly, A. E. Davletov, S. Syzganbaeva, V. V. Voronkov, and I. M. Tkachenko, Contrib. Plasma Phys. **55**, 381 (2015); for more details see Yu. V. Arkhipov, A. B. Ashikbayeva, A. Askaruly, A. E. Davletov, and I. M. Tkachenko, Phys. Rev. E **90**, 053102 (2014); Yu. V. Arkhipov, A. B. Ashikbayeva, A. Askaruly, A. E. Davletov, and I. M. Tkachenko, Phys. Rev. E **91**, 019903 (2015).

[15] V. I. Perel' and G. M. Eliashberg, Zh. Eksp. Teor. Fiz. **41**, 886 (1961) Sov. Phys. JETP **14**, 633 (1962).

[16] P. Magyar, Z. Donkó, G. J. Kalman, and K. I. Golden, in *15th International Conference on the Physics of Non-Ideal Plasmas (Almaty, 2015)*, p. 52; for more details see P. Magyar, Z. Donkó, G. J. Kalman, and K. I. Golden, Phys. Rev. E **90**, 023102 (2014).

[17] S. Ichimaru, *Statistical Plasma Physics* (Addison-Wesley, New York, 1994), Vol. II.

[18] I. M. Tkachenko, in *International Conference on Operator Theory and its Applications in Mathematical Physics* (Stefan Banach International Mathematical Center, Będlewo, 2002), p. 20.

[19] V. M. Adamyan, T. Mayer, and I. M. Tkachenko, Fiz. Plazmy **11**, 826 (1985) Sov. J. Plasma Phys. **11**, 481 (1985).
[20] R. P. Feynman, Phys. Rev. **94**, 262 (1954).
[21] G. J. Kalman, S. Kyrkos, K. I. Golden, P. Hartmann, and Z. Donko, Contrib. Plasma Phys. **52**, 219 (2012); Europhys. Lett. **90**, 55002 (2010); V. B. Bobrov, S. A. Trigger, and D. I. Litinski, arXiv:1407.6184.
[22] J. Vorberger, Z. Donko, I. M. Tkachenko, and D. O. Gericke, Phys. Rev. Lett. **109**, 225001 (2012).
[23] J. W. Eastwood, R. W. Hockney, and D. N. Lawrence, Comput. Phys. Commun. **19**, 215 (1980).
[24] See Supplemental Material at http://link.aps.org/supplemental/10.1103/PhysRevLett.119.045001 for additional graphical results, which includes Refs. [25–32].
[25] I. Z. Fisher, *Statistical Theory of Liquids* (University of Chicago Press, Chicago, 1964).
[26] K. Ng, J. Chem. Phys. **61**, 2680 (1974).
[27] Y. Rosenfeld and N. W. Ashcroft, Phys. Rev. A **20**, 1208 (1979).
[28] M. S. Wertheim, Phys. Rev. Lett. **10**, 321 (1963).
[29] G. Faussurier and M. S. Murillo, Phys. Rev. E **67**, 046404 (2003).
[30] D. A. Young, E. M. Corey, and H. E. DeWitt, Phys. Rev. A **44**, 6508 (1991).
[31] N. Desbiens, P. Arnault, and J. Clérouin, Phys. Plasmas **23**, 092120 (2016).
[32] J.-P. Hansen, I. R. McDonald, and E. L. Pollock, Phys. Rev. A **11**, 1025 (1975).
[33] J. P. Mithen, J. Daligault, B. J. B. Crowley, and G. Gregori, Phys. Rev. E **84**, 046401 (2011).
[34] S. V. Adamjan and I. M. Tkachenko, Ukr. Fiz. Zh. **36**, 1336 (1991). The translation of this article can be provided on request by the corresponding author.
[35] J. Ortner and I. M. Tkachenko, Phys. Rev. A **46**, 7882 (1992).
[36] J. Ortner, Phys. Scr. **T84**, 69 (2000).